

Koopman mode analysis on thermal data for building energy assessment

Ljuboslav Boskic , Cory N. Brown & Igor Mezić

To cite this article: Ljuboslav Boskic , Cory N. Brown & Igor Mezić (2020): Koopman mode analysis on thermal data for building energy assessment, Advances in Building Energy Research, DOI: [10.1080/17512549.2020.1842802](https://doi.org/10.1080/17512549.2020.1842802)

To link to this article: <https://doi.org/10.1080/17512549.2020.1842802>



Published online: 11 Nov 2020.



Submit your article to this journal [↗](#)



Article views: 132



View related articles [↗](#)



View Crossmark data [↗](#)



Koopman mode analysis on thermal data for building energy assessment

Ljuboslav Boskic, Cory N. Brown and Igor Mezić

Department of Mechanical Engineering, University of California Santa Barbara, Santa Barbara, CA, USA

ABSTRACT

Current approaches to thermal control and energy management in residential and office buildings rely on complex or high-dimensional thermal models. We provide a means to extract features from in-office thermal-data sensors which avoid the use of standard models. We develop these data-driven methods through the use of Koopman operator theory. We validate our resulting algorithms via analysing thermal data from a single thermal zone space. The particular advantage of the method is that it associates the temporal characteristics of control mechanisms with the corresponding spatial zones of influence. The methodology enables identification of spatial heating and cooling control modes directly from the data.

ARTICLE HISTORY

Received 6 December 2019
Accepted 6 October 2020

KEYWORDS

Koopman mode decomposition; data-driven energy management; office space energy management; residential space energy management; building energy

1. Introduction

The ‘House as a System’ approach is gaining traction as a protocol to gain deep energy efficiency in residential buildings (Hoicka & Parker, 2018). However, the current approach is focused on scheduling the order of retrofits (insulation first, replacement of furnace second, etc.) and thus high capital expenditure actions. In commercial buildings, the cost of such retrofits has led to development of strategies for optimising operations of existing systems, focusing first on fault detection and returning the building operation to a ‘healthy’ state (Littooy et al., 2016). Beyond the fault detection methodologies, model-based approaches lead to optimisation of existing systems and potential of deep energy savings for new commercial builds (Georgescu & Mezić, 2015), and even US Army facilities (Mezic, 2017). However, these gains are not currently utilised in the context of residential buildings or individual office spaces.

Therefore, residential buildings and individually managed office spaces have recently gained more attention within the topic of energy efficiency. There are about 136.5 million residential buildings in the United States (Bureau, 2018), creating a large opportunity for energy savings via retrofits and new designs, to create more efficient homes. Through addition of sensing, communication and actuation of components, devices are made ‘smart’, such that they communicate wirelessly with each other and transmit data to help reduce use during peak demand periods. Smart home and office technologies have potential to deliver benefits such as convenience, control, security and monitoring,

environmental protection, and enjoyment from engaging with the technology itself (Ford et al., 2017). Current control methodologies rely on models with complex physics and uncertainty in parameters that hamper performance and implementation. Here we introduce a data-driven (model-independent) methodology for indoor temperature of a single zone and multi-zone buildings, with the goal of improving energy efficiency for residential buildings or individual office spaces that can serve as a basis for energy saving algorithms. Some initial work has been done in finding a physical model to help with these energy saving algorithms for residential buildings (Boskic & Mezić, 2020). This model independence is achieved through the use of Koopman operator methods in the design of unsupervised learning algorithms.

The Koopman operator is an infinite-dimensional, linear operator that acts on a Hilbert space of functions called the space of observables (Koopman & Neumann, 1932; Koopman, 1931). The eigenvalues and eigenfunctions of this linear operator are capable of capturing key characteristics of the dynamical system which we assume we are observing in the generation of any time series of interest. Additionally, the Koopman modes, corresponding to a particular choice of observable function, allow one to reconstruct and forecast (predict) the observed quantities. Together, Koopman eigenvalues, eigenfunctions, and modes yield the Koopman mode decomposition (KMD) of an arbitrary observable (Arbabi & Mezić, 2017b; Mezić, 2005). Koopman modes, under our choice of observables, identify spatial domains (zones) associated with specific temporal dynamics, thus enabling, for example, spatial zones of interest for actuation in optimal control strategies. KMD has been used in various fields such as fluid flow (Rowley et al., 2009), biology (Hasnain et al., 2019), and traffic networks (Avila & Mezić, 2020).

To enable Koopman mode analysis, we have collected temperature readings at five locations within our Laboratory at UCSB and an outdoor reading from the Santa Barbara Municipal Airport (~2 miles away). In addition, we also have humidity, light, pressure, and noise measurements for the indoor sensors. Measurements from these sensors (along with outdoor temperature) taken every 5 min over the course of 5 days can be found in Figure 4.

The paper is organised as follows: In Section 2, we describe the sensor implementation (data collection). In Section 3, we describe the basics of data-driven Koopman spectral analysis. In Section 4, we describe the results of the analysis using the Koopman operator theory. We conclude in Section 5.

2. Sensor implementation

In order to understand effect of occupancy patterns on temperature variations, we have incorporated Omron Environment Sensors into our laboratory space. In this section, we describe their implementation and data analytics.

Figure 1 shows the full schematic of an individual sensor. The sensors detect temperature, humidity, light, UV index, pressure, and sound in one compact package. Bluetooth is used to sync the data with a cell phone. The data was collected on 5-minute intervals, for the period May 6th 0:00 to May 11th 0:00, and stored in a CSV file. The outdoor temperature was gathered from the National Weather Service, taken by Santa Barbara Municipal Airport, which is in close proximity to the laboratory space. The placement of five sensors is shown in Figure 2 and a schematic along with the HVAC vents is shown in Figure 3. We

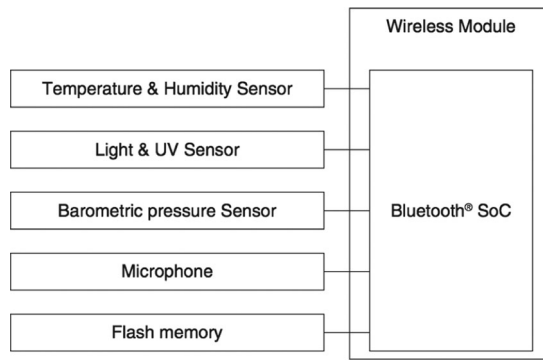


Figure 1. Block diagram of the Omron sensor module (Environment Sensor, 2018).

keep the sensors at similar heights and away from direct HVAC vents. We also try to keep the sensors at a reasonable distance away from light sources and any pipes that may radiate heat.

As an example of data timetraces, in [Figure 4](#), we show the plot of the five sensors and the outdoor temperature in degrees Celsius. Several interesting features are observable. The 24 h (daily) dynamics of the outdoor temperature is somewhat reflected in the room dynamics. However, there are short-term oscillations in the room temperature that are not present in the outdoor temperature data and are clearly due to control dynamics. These are particularly visible in the 4th and 5th day of observation.

3. Koopman mode decomposition

In the context of deterministic dynamical systems, state-variables are those variables that if known for a system at a particular time, the dynamics of the system would be determined for all of time (e.g. use angle and angular velocity for the mathematical pendulum). The classical approach in dynamical systems theory is to work in a mathematical space in which variables which describe the current state of the system are the main objects of interest, i.e. state-space. When recording dynamic data from complex systems such as buildings, the state variables which fully describe the system are not known and there may be too many to ever measure. This poses no problem for the operator theoretic view of dynamical systems in which the main objects of interest are functions whose domain are the state-space – known as *observables* (Budišić et al., 2012). In the case of the pendulum, this could be kinetic energy, potential energy, or another function of angle and angular momentum. In this view, we can think of any measurements (or possibly functions of measurements) we take of a system of interest as a function of some unknown state. In the context of buildings, the states could be temperature, light, noise, humidity. It is convenient to have access to spatially distributed measurements, as the spatial features and control mechanisms can be analysed. We pursue this here.

The simplest context in which to introduce the Koopman view is for discrete-time dynamical systems which can be described by repeated application of a single function $T: M \rightarrow M$, i.e.

$$x' = T(x) \quad (1)$$

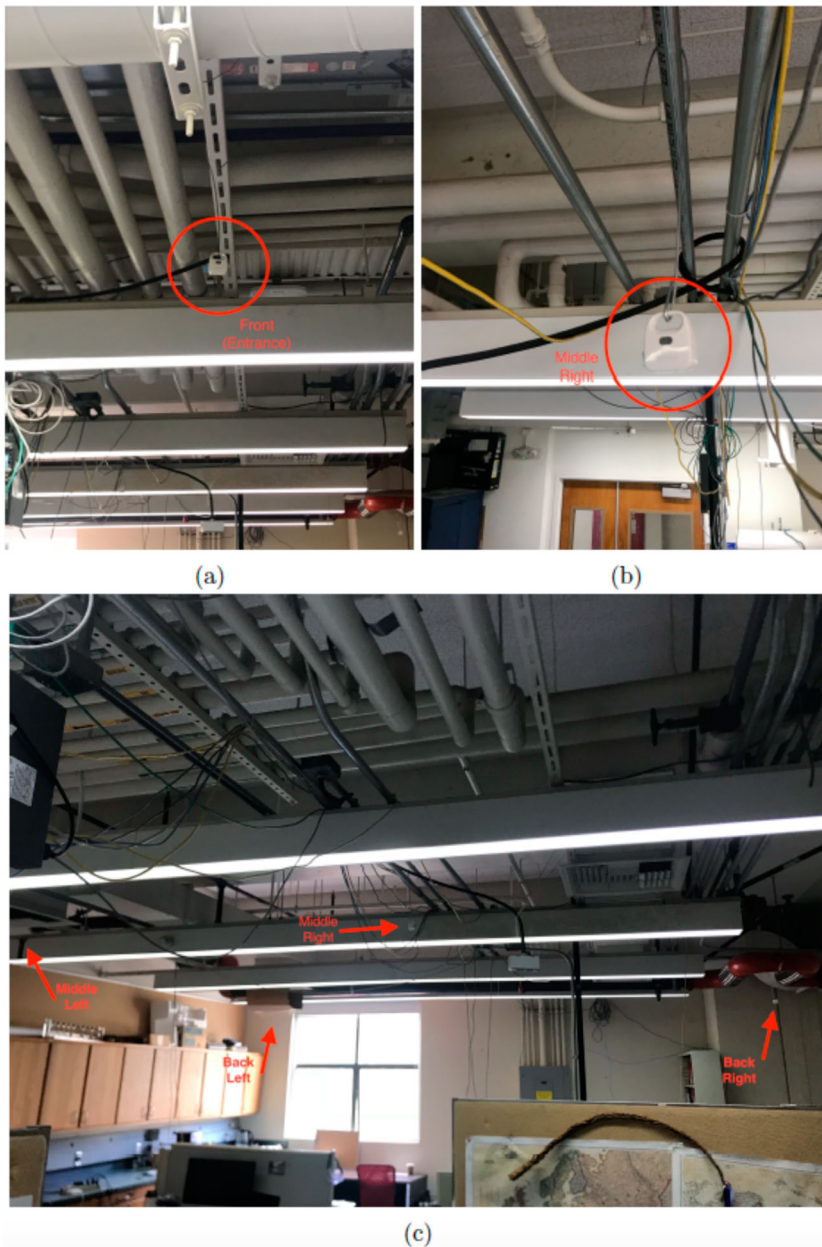


Figure 2. Sensor placement within the office. (a) shows the front sensor close to the entrance the office. (b) shows the sensor in the middle part of the office labelled as middle right, and the location in respect to the entrance door (c) shows the general placement of the other sensors and their corresponding names.

Assume M is any set whose elements label all possible states (e.g. state-space for the logistic map) of the system and x' is the updated state, corresponding to x , after a single time step. The Koopman operator framework was originally described for Hamiltonian vector fields on manifolds (generalized setting of Hamiltonian systems of ordinary differential equations) (Koopman, 1931) and has been extended to the case of stochastic (Mezić,

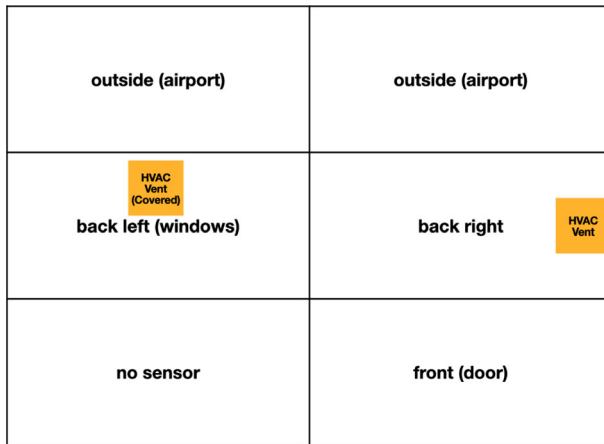


Figure 3. Sensor placement schematic along with HVAC vents.

2005; Mezić & Banaszuk, 2004) and nonautonomous (Maćešić et al., 2017) systems. For the dynamical system described by equation (1), the induced Koopman operator U represents a new discrete-time dynamical system whose state-space is the set of all complex-valued observables with domain M (denoted by \mathbb{C}^M):

$$f' = U(f) = f \circ T \quad (\circ \text{ is function composition}).$$

It is easy to show that U is linear ($c \in \mathbb{C}$ and $f, g \in \mathbb{C}^M$),

$$U(cf + g) = (cf + g) \circ T = c(f \circ T) + g \circ T = cU(f) + U(g),$$

thus we can consider eigenvalues λ and eigenfunctions ϕ ,

$$U(\phi) = \lambda\phi.$$

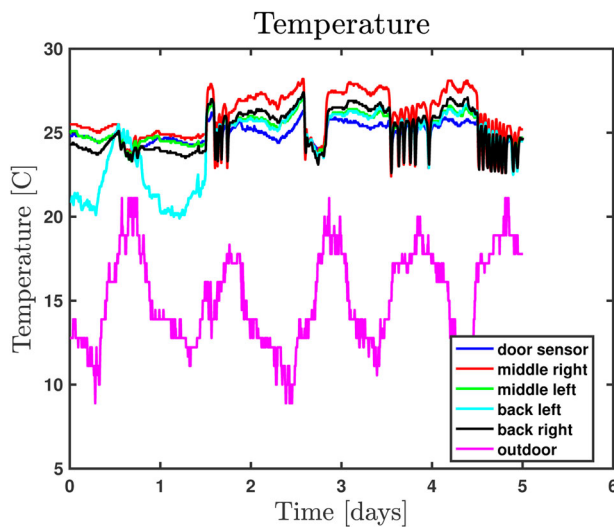


Figure 4. Temperature traces from five indoor sensors and the outdoor sensor, utilised on Koopman Mode Analysis.

Research into the spectral expansion of the Koopman operator for data-driven analysis of dynamical systems was initiated by Mezić (2005); Mezić and Banaszuk (2004).

Considering the repeated action of U , p times, on a finite collection of n observables $\{f_1, \dots, f_n\}$ that lie in the span of a finite collection of m eigenfunctions $\{\phi_1, \dots, \phi_m\}$, with eigenvalues $\{\lambda_1, \dots, \lambda_m\}$ and dual basis $\{\psi_1, \dots, \psi_n\}$, leads to a special case of the Koopman mode decomposition (KMD):

$$\begin{bmatrix} U^p(f_1) \\ \vdots \\ U^p(f_n) \end{bmatrix} = \begin{bmatrix} \sum_{k=1}^m \lambda_k^p \phi_k \psi_k(f_1) \\ \vdots \\ \sum_{k=1}^m \lambda_k^p \phi_k \psi_k(f_n) \end{bmatrix} = \sum_{k=1}^m \lambda_k^p \phi_k \begin{bmatrix} \psi_k(f_1) \\ \vdots \\ \psi_k(f_n) \end{bmatrix}. \quad (2)$$

This decomposition allows us to evolve observables $\{f_1, \dots, f_n\}$ by simply multiplying each term in the sum above by its corresponding eigenvalue λ_k . This enables the intuitive interpretations of the magnitude and complex phase of λ_k as corresponding to rate of growth and frequency of oscillation, respectively. If we are only interested in the evolution of the observables along a single trajectory of (1) starting at x , then the ϕ_k 's could be chosen so that $\phi_k(x) = 1$, and KMD would take the following simpler form

$$\begin{bmatrix} [U^p(f_1)](x) \\ \vdots \\ [U^p(f_n)](x) \end{bmatrix} = \begin{bmatrix} \sum_{k=1}^m \lambda_k^p \phi_k(x) \psi_k(f_1) \\ \vdots \\ \sum_{k=1}^m \lambda_k^p \phi_k(x) \psi_k(f_n) \end{bmatrix} = \sum_{k=1}^m \lambda_k^p \begin{bmatrix} \psi_k(f_1) \\ \vdots \\ \psi_k(f_n) \end{bmatrix}. \quad (3)$$

3.1. Dynamic mode decomposition

The last column vector appearing in (2) and (3) is known as the Koopman Mode of the observables $\{f_1, \dots, f_n\}$ relative to the discrete-time system described by (1). From (3), we see that the magnitude of $\psi_k(f_i)$ tells us how much of a role the growth and oscillations rates given by λ_k play a role in evolution of f_i along the single trajectory starting at x . Similarly, the complex phase of $\psi_k(f_i)$ gives a relative phase corresponding to the oscillations give by λ_k .

The most common approximation of the Koopman operator and its spectral quantities is given by the Dynamic Mode Decomposition (DMD) (Arbabi & Mezić, 2017a; Klus, 2016; Korda & Mezić, 2018; Mezić & Arbabi, 2017; Schmid, 2010; Williams et al., 2015), we have used it on building data; first we give a brief description of DMD.

Consider the case where we have a discrete-time dynamical system as in (1) and we have evaluated a set of observables $\{f_1, \dots, f_n\}$ along the first $m+1$ time points of a trajectory starting at x . We can put this into a matrix D such that each row corresponds to a different observable and the columns are ordered by time:

$$D = \begin{bmatrix} f_1(x) & f_1(T(x)) & \dots & f_1(T^m(x)) \\ \vdots & \vdots & \ddots & \vdots \\ f_n(x) & f_n(T(x)) & \dots & f_n(T^m(x)) \end{bmatrix} \quad (4)$$

$$= \begin{bmatrix} f_1(x) & [U(f_1)](x) & \dots & [U^m(f_1)](x) \\ \vdots & \vdots & \ddots & \vdots \\ f_n(x) & [U(f_n)](x) & \dots & [U^m(f_n)](x) \end{bmatrix}. \quad (5)$$

We can split D into the matrix X of the first m columns and Y of the last m columns, i.e.

$$X = \begin{bmatrix} f_1(x) & f_1(T(x)) & \dots & f_1(T^{m-1}(x)) \\ \vdots & \vdots & \ddots & \vdots \\ f_n(x) & f_n(T(x)) & \dots & f_n(T^{m-1}(x)) \end{bmatrix}, \quad (6)$$

$$Y = \begin{bmatrix} f_1(T(x)) & f_1(T^2(x)) & \dots & f_1(T^m(x)) \\ \vdots & \vdots & \ddots & \vdots \\ f_n(T(x)) & f_n(T^2(x)) & \dots & f_n(T^m(x)) \end{bmatrix}. \quad (7)$$

The main idea in DMD is to find a matrix A such that AX is close to Y in some sense. In this way, A would be mapping the vector of samples taken at the point $T^i(x)$ close to those taken at the point $T^{i+1}(x)$, for all $i \in \{0, \dots, m-1\}$. Intuitively, as the number of time points goes to infinity or as we add more observables (which could just be functions of our original ones), we should better and better approximate the Koopman operator U by the linear operator we are representing by the matrix A . One such A we could use is $A = YX^\dagger$, where X^\dagger is the pseudo-inverse of X . Such an A satisfies the following (Boyd & Vandenberghe, 2004):

$$\|AX - Y\|_F = \inf_{B \in \mathbb{R}^{m \times n}} \|BX - Y\|_F.$$

If we let $M = \mathbb{R}^n$ and $T(x) = Ax$ as in Equation (1), then DMD of the data matrix D approximates KMD of the functions $\{f_1, \dots, f_n\}$ with respect to the system described by Equation (1).

3.2. DMD rank reduction

The Koopman Operator is an infinite-dimensional operator. However, when low-dimensional structures in the underlying physics exist, they can be captured with a few modes. An efficient approach to this computes DMD modes in the basis of U that is taken from an singular value decomposition (SVD) of the data matrix X (Brunton et al., 2016).

In order to truncate DMD algorithms with r modes, we will use a truncated SVD basis where we keep the r largest singular values. In order to select r , we examine the singular values on the diagonal of S . We select r such that the sum of the first r singular values accounts for over 95% of the variance in the data.

Algorithm 1 Hankel Power Spectrum DMD

Consider data matrix D as defined (4).

1. Define hankel matrices X and Y as in (6) and (7) with n delays.
2. Compute the SVD of X :

$$\text{svd}(X) = US\tilde{V}^*$$

3. Find dimension of subspace and truncate as discussed in 3.2.

4. Form the matrix

$$\tilde{A} = S^{-\frac{1}{2}} U^* Y \tilde{V} S^{-\frac{1}{2}}$$

5. Compute eigendecomposition of \tilde{A} . Let $(\lambda_j, \tilde{w}_j), j = 1, 2, \dots, m$, be the eigenvalue-vector pair. The eigenvalue of \tilde{A} is identical to the eigenvalue of A , and

$$W = S^{\frac{1}{2}} \tilde{W}$$

are the eigenvectors of \tilde{A} . These eigenvectors are scaled so they do not have unit norm.

6. The dynamic modes ψ_j are defined as

$$\psi_j = Y V S^{-1} W$$

7. Define f to be the frequency of the oscillation to be

$$f_i = \frac{\text{Im}(\log(\lambda_i)) / \Delta T}{2\pi}$$

8. Lastly define the Power to be square of the magnitude of the modes

$$P = \|\psi\|^2$$

4. Analysis and results

In the following, we perform Koopman spectral analysis on the temperature data in [Figure 4](#) via the use of DMD algorithm discussed above. We assign a ‘power’ that each DMD mode represents in the data matrix X . Since the algorithm involves inverses of the diagonal matrix of singular values of X , we treat any singular value less than $\sigma/10^6$ as zero, where σ is the largest singular value.

4.1. Dynamic mode decomposition on temperature data

As observables, we use the temperature measured at 5 different points in the office and the local outdoor temperature. We denote these by $\{f_1, \dots, f_6\}$. Their timetraces are shown in [Figure 4](#). It is noticeable that indoor sensors have similar responses to control, with the exception of the back left space in the first couple of days.

Since we have only six observables, and data sampling at 5 min intervals, we have a very ‘fat’ matrix D – an underdetermined system. The data matrix used in this analysis is of size $[6 \times 1441]$. Thus we use a Hankel matrix that gives us a delayed embedding of the data ([Arbabi & Mezić, 2017a](#)). We also use time-shifted versions of these observables to generate new ones, e.g. by $f_7 = f_1 \circ T$. We will augment our data with 200 delays which will give result in an X and Y matrix to be of size $[1206 \times 1240]$. Since our system is a underdetermined system due to the size of original data matrix, we try to find an optimal amount of time delays used for the augmentation of the X and Y matrix. For this we, use the following relative error:

$$\frac{\tilde{A}X - Y_F}{Y_F}. \quad (8)$$

In the following figures, we have several plots representing Koopman spectral quantities related to the observables. In [Figures 5](#) and [6](#), we use 200 and 300, respectively, time

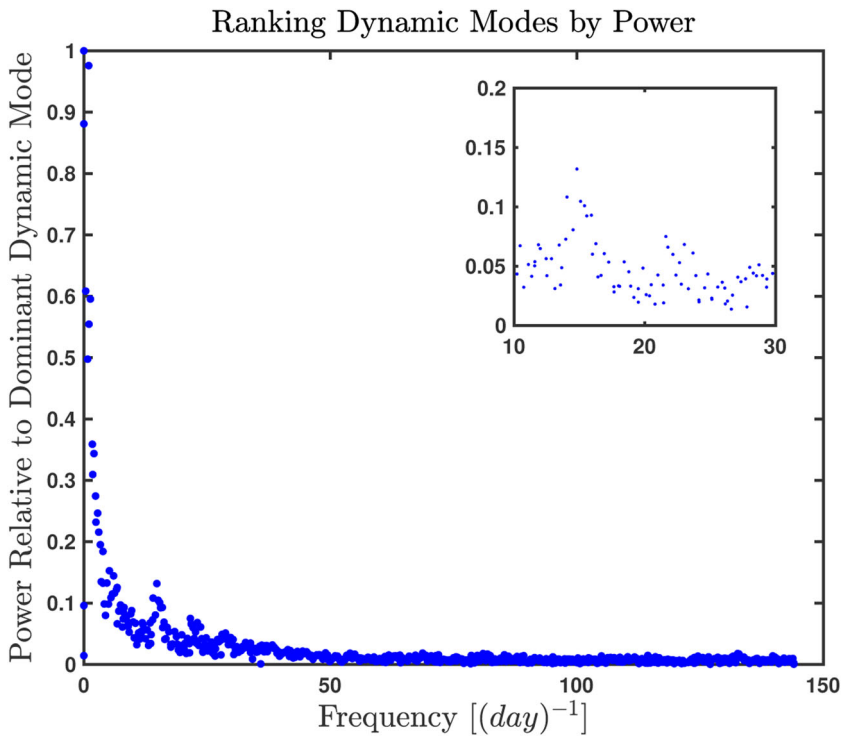


Figure 5. Plot of dynamic mode ranking against frequency with 200 delays for the augmented data. Frequency 1 day^{-1} and 15 day^{-1} are of particular interest showing the highest 'power'. Due to the sorting of the dynamic modes, we find mode 3 and 43 are corresponding to frequency 1 day^{-1} and 15 day^{-1} , respectively.

shifted observables for each of our six temperature sensors, using the information from [Figure 7](#), that shows the relative error compared to the number of delays used in the Hankel matrix. Relative error was computed using Equation (8). Something to note from this is more delays is sometimes not optimal, i.e. can be considered as over training the system by giving it more states than needed to perform the analysis.

The eigenvalues values mostly lie on the unit disk, with a few having some with larger imaginary part meaning oscillations as seen in [Figure 8](#). The mode with frequency near day^{-1} has much larger magnitude for the outside component than for any inside component. This is expected, since indoor temperature is more stable due to control. The bumps in the frequency plot near frequencies of 15 day^{-1} and 25 day^{-1} are another consistent feature amongst the plots for different numbers of time-shifted observables. We will use the frequency of 15 day^{-1} for further evaluation since we have some intuition of what might be the cause of the interesting dynamics. This mode, having a period near 1.5 h, has much larger components indoor than outdoor, and is related to heating and cooling control.

The plots, [Figures 5 and 6](#), contains the frequency of each DMD eigenvalue with its power. We are plotting these in units of day^{-1} . Notice the two bumps in the spectrum [Figure 5](#) around a frequency of 15 day^{-1} and 25 day^{-1} , these frequencies correspond

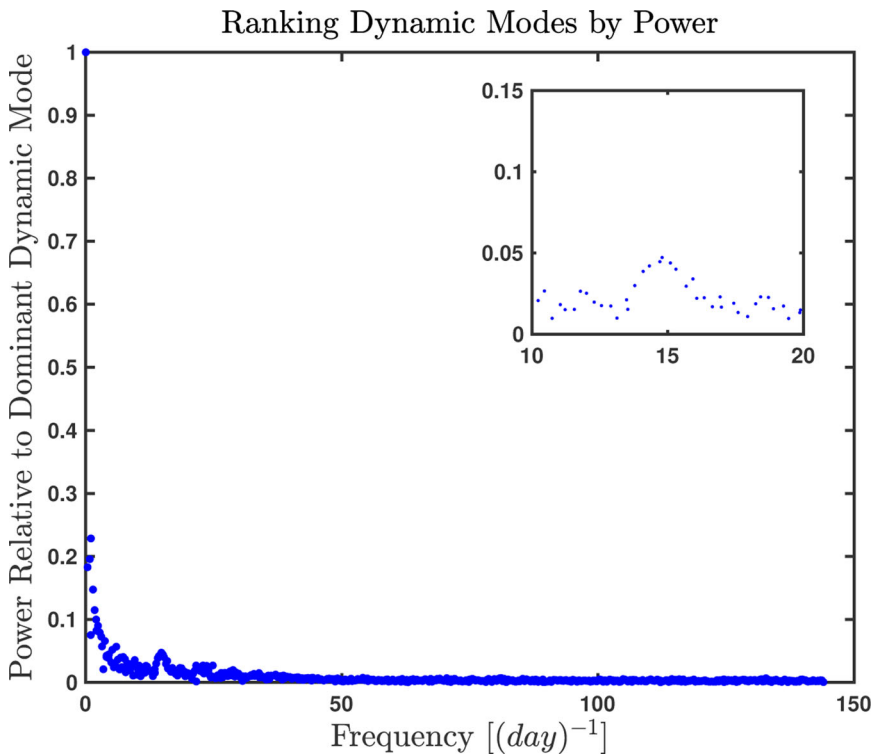


Figure 6. Plot of dynamic mode ranking against frequency with 300 delays for the augmented data. Again showing frequency 1 day^{-1} and 15 day^{-1} . Due to the sorting of the dynamic modes, we find mode 4 and 34 are corresponding to frequency 1 day^{-1} and 15 day^{-1} , respectively.

to control action. This control action is set to have cooling come on every 1.5 h and this can even be seen in Figure 4 where day 0 and 1 are controlled to be between a certain temperature inside the space during work hours. Figures 9 and 10 contains a representation of the first six components of the highest power DMD mode with frequency close to one, corresponding to the daily cycle. The magnitude (left) and complex phase (right) of each of the components of this mode are represented using colours over a simplified diagram of our office. The magnitudes are relatively uniform, indicating the ability of control to largely achieve the objective. Notice that the phase of $-\pi$ is equal to π explaining the difference in colour seen in the figure.

Figures 11 and 12 represents the highest power mode with frequency near 15 day^{-1} . The outside sensor shows no magnitude at this frequency, implying the mode is due to the control action. With this analysis, we can determine that the interesting dynamics are occurring in a particular part of the office space. We are also able to confirm this analysis since we know in particular a HVAC vent exists to the right of the sensor. Another interesting observation pulled from the phase of the mode of the back left sensor is we can see that area is not uniform with the rest of the room but also not 1 radian out of phase like the middle right. If we notice in Figure 2, the back left sensor also has a HVAC vent but there is cardboard blocking the airflow out. This caused the analysis to pick up little control action since there was an obstruction.

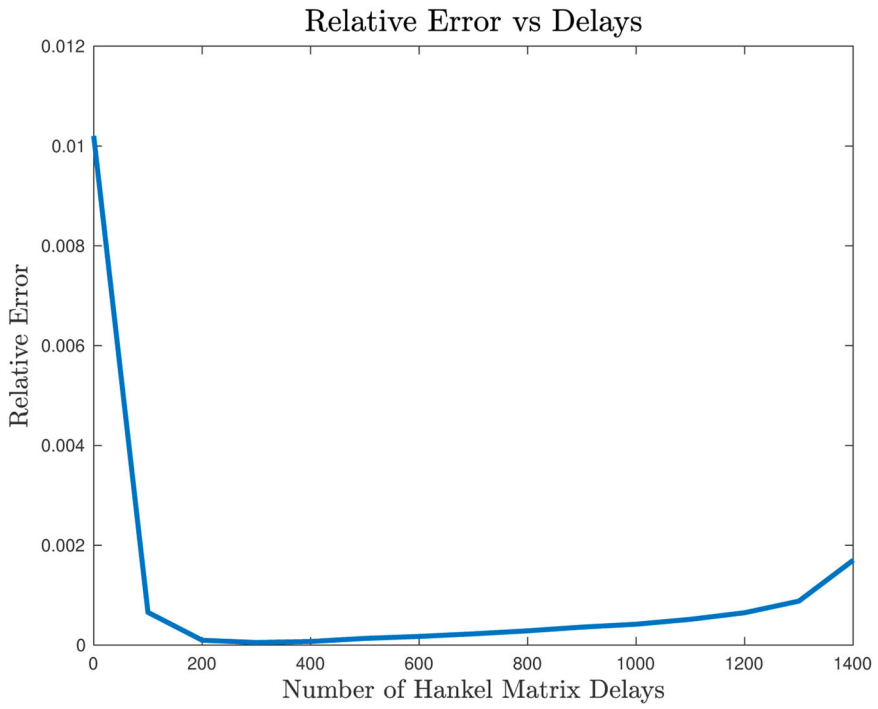


Figure 7. Relative error compared to the amount of time delays used for the augmented data.

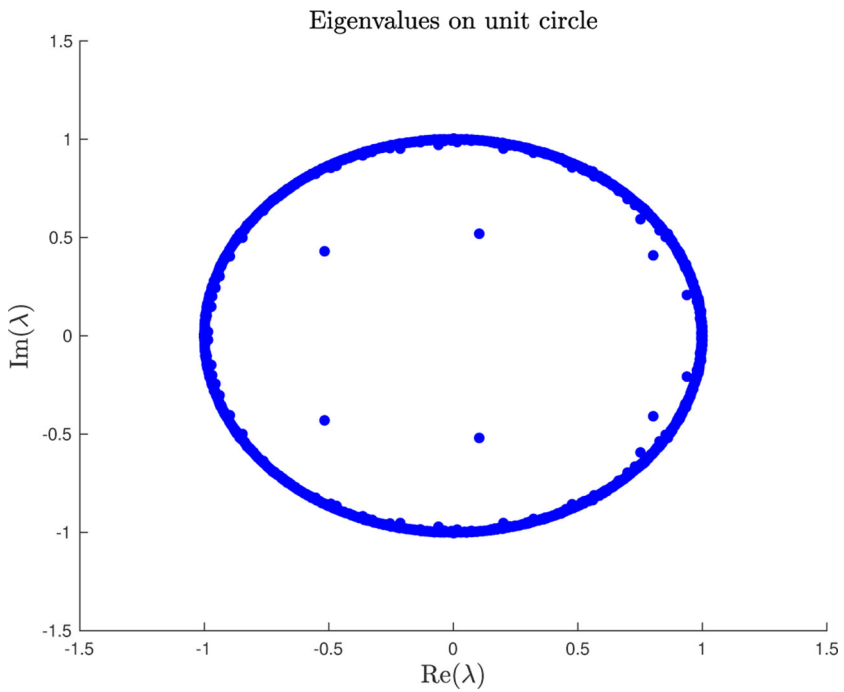


Figure 8. Plot of real and imaginary eigenvalues using the 300 delays for the augmented data.

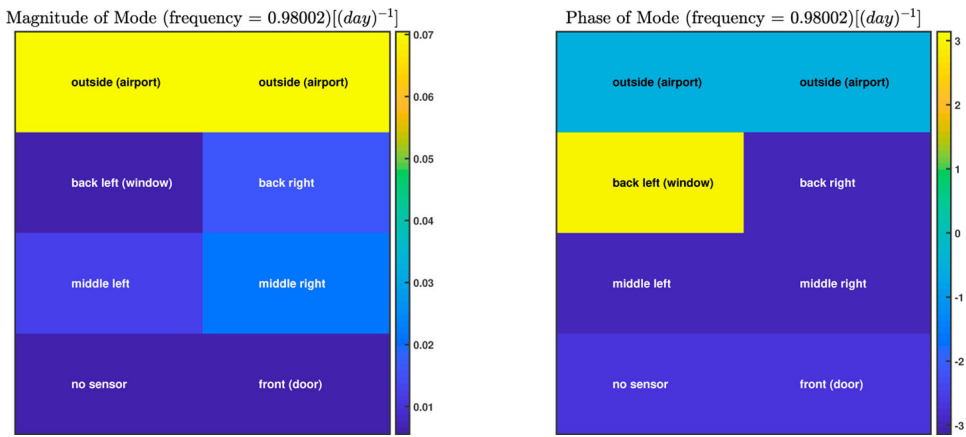


Figure 9. Plotting mode 3 which has a period of 1 per day. The magnitude of the mode shows which part of the office affects the dynamics the most and phase of mode shows how different locations act in and our phase with each other.

It is remarkable that this is an emergent feature of the control system. Namely, the frequency of oscillation is not built into the control software but emerges from the operation of the system. This observation can be used for correct tuning of control systems using Koopman Mode Analysis. Visible are also differences in magnitude of this mode, indicating different local conditions for different spatial locations. This is also useful information for understanding of operation of an implemented control system. The phases of the mode show uniformity.

The analysis using Koopman modes gives us a insight into the thermal dynamics of indoor spaces. Namely, the distinction between the zones affected strongly by the outside conditions, near the window, are evident. In addition, there are modes that clearly indicate dynamics of the controllers. In this way, the external influences are separated from control dynamics.

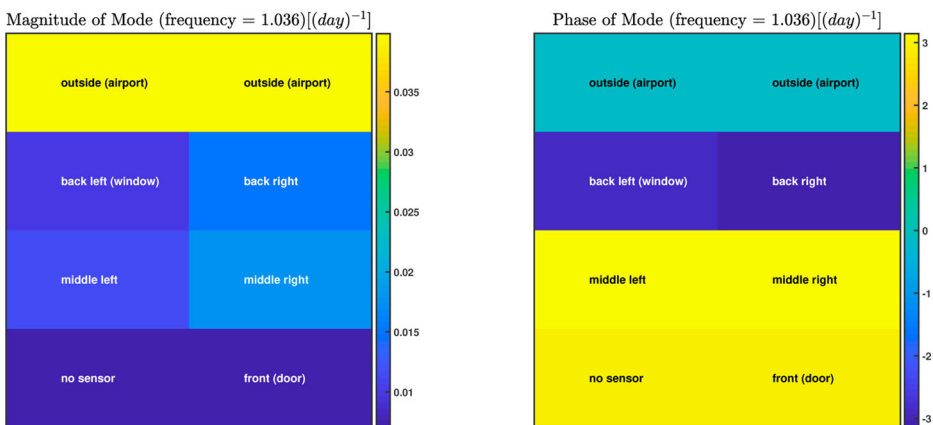


Figure 10. Plotting mode 4 which has a period of 1 per day.

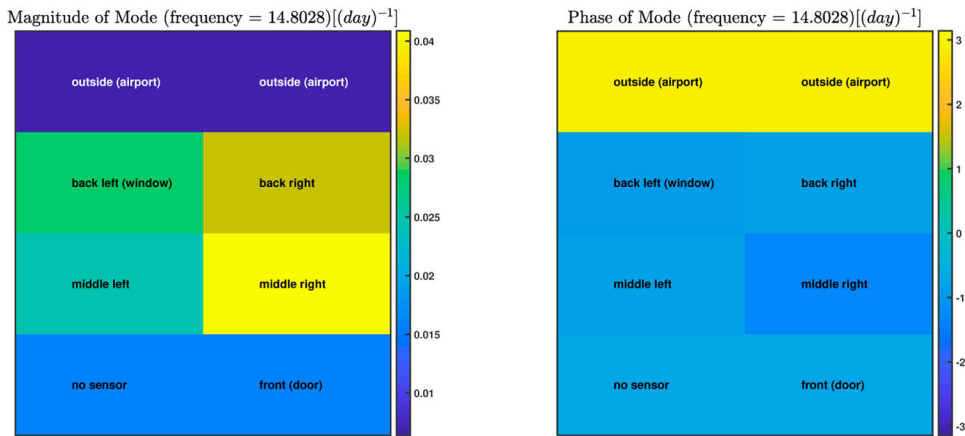


Figure 11. Plotting mode 43 which has a period of 1.5 h. The magnitude of the mode shows that the middle right sensor has the most interesting dynamics related to this period of evaluation. As well as the same location being out of phase with the rest of the office space.

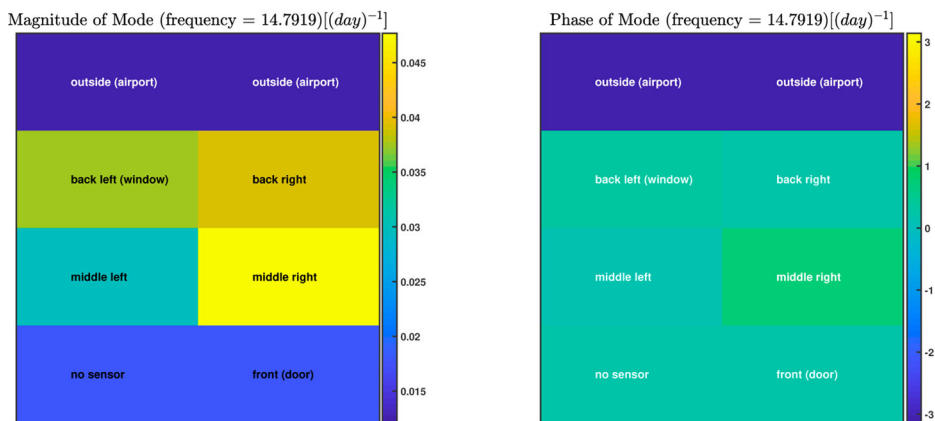


Figure 12. Plotting mode 34 which has a period of 1.5 h. The magnitude of the mode shows that the middle right sensor has the most interesting dynamics again.

5. Conclusions

In this paper, we described the utilisation of Koopman mode analysis for determination of emergent properties of air conditioning control systems in individual office spaces or residential buildings. Due to having a small number of raw experimental observables, yet good temporal resolution, the Hankel DMD method was applied to approximate spectral properties of the Koopman operator directly from data. Thermal control algorithms possess emergent properties and spatial inhomogeneities that can be detected using the data-driven Koopman Mode Analysis. In the office space, we studied a thermal mode with an oscillatory period of 1.5 h was detected, clearly driven by control action, enabling for the first time spatial and temporal analysis of the oscillatory control behaviour directly from data. Inhomogeneities in spatial control action were determined based

on the magnitude and phase of the mode associated with the 1.5 h period of oscillation. The layout of the sensors and HVAC vent placement was seen in Figure 3 which confirms the DMD analysis discussed above.

The results can be used for tuning control systems to obtain better control action as well as energy efficiency. The method also provides insights into the design of actuation, as spatial inhomogeneities in modes are typically connected to location of air diffusers. The analysis presented here is not restricted to temperature data. Humidity, as well as sound (noise pollution) can be studied using the same methodology.

Acknowledgments

The authors would like to thank Jim and Beverly Zaleski for making this work possible.

Disclosure statement

No potential conflict of interest was reported by the author(s).

Funding

This research was made possible by the generous gift from the Zaleski Foundation.

References

- Arbabi, H., & Mezić, I. (2017a). Ergodic theory, dynamic mode decomposition, and computation of spectral properties of the Koopman operator. *SIAM Journal on Applied Dynamical Systems*, 16(4), 2096–2126. <https://doi.org/10.1137/17M1125236>
- Arbabi, H., & Mezić, I. (2017b). Study of dynamics in post-transient flows using Koopman mode decomposition. *Physical Review Fluids*, 2(12), 124402. <https://doi.org/10.1103/PhysRevFluids.2.124402>
- Avila, A. M., & Mezić, I. (2020). Data-driven analysis and forecasting of highway traffic dynamics. *Nature Communications*, 11(1), 2090. <https://doi.org/10.1038/s41467-020-15582-5>
- Boskic, L., & Mezić, I. (2020). Control-oriented, data-driven models of thermal dynamics.
- Boyd, S., & Vandenberghe, L. (2004). *Convex optimization*. Cambridge University Press.
- Brunton, B. W., Johnson, L. A., Ojemann, J. G., & Kutz, J. N. (2016). Extracting spatial-temporal coherent patterns in large-scale neural recordings using dynamic mode decomposition. *Journal of Neuroscience Methods*, 258, 1–15. <https://doi.org/10.1016/j.jneumeth.2015.10.010>
- Budišić, M., Mohr, R., & Mezić, I. (2012). Applied koopmanism. *Chaos: An Interdisciplinary Journal of Nonlinear Science*, 22(4), 047510. <https://doi.org/10.1063/1.4772195>
- Bureau, U. S. C. (2018). Number of housing units in the United States from 1975 to 2017 [Computer software manual]. <https://www.statista.com/statistics/240267/number-of-housing-units-in-the-united-states/>
- Environment Sensor (2008). Environment Sensor (Computer software manual No. 2JCIE-BL01).
- Ford, R., Pritoni, M., Sanguinetti, A., & Karlin, B. (2017). Categories and functionality of smart home technology for energy management. *Building and Environment*, 123, 543–554. <https://doi.org/10.1016/j.buildenv.2017.07.020>
- Georgescu, M., & Mezić, I. (2015). Building energy modeling: A systematic approach to zoning and model reduction using Koopman mode analysis. *Energy and Buildings*, 86, 794–802. <https://doi.org/10.1016/j.enbuild.2014.10.046>
- Hasnain, A., Boddupalli, N., & Yeung, E. (2019). Optimal reporter placement in sparsely measured genetic networks using the Koopman operator. arXiv preprint arXiv:1906.00944.

- Hoicka, C. E., & Parker, P. (2018). Assessing the adoption of the house as a system approach to residential energy efficiency programs. *Energy Efficiency*, 11(2), 295–313. <https://doi.org/10.1007/s12053-017-9564-x>
- Klus, E. A. (2016, 09). On the numerical approximation of the Perron-Frobenius and Koopman operator. *Journal of Computational Dynamics*, 3, 51–79. <https://doi.org/10.3934/jcd.2016003>
- Koopman, B., & Neumann, J. V. (1932). Dynamical systems of continuous spectra. *Proceedings of the National Academy of Sciences*, 18(3), 255–263. <https://doi.org/10.1073/pnas.18.3.255>
- Koopman, B. O. (1931). Hamiltonian systems and transformation in Hilbert space. *Proceedings of the National Academy of Sciences*, 17(5), 315–318. <https://doi.org/10.1073/pnas.17.5.315>
- Korda, M., & Mezić, I. (2018, April 01). On convergence of extended dynamic mode decomposition to the Koopman operator. *Journal of Nonlinear Science*, 28(2), 687–710. <https://doi.org/10.1007/s00332-017-9423-0>
- Littooy, B., Loire, S., Georgescu, M., & Mezić, I. (2016). Pattern recognition and classification of HVAC rule-based faults in commercial buildings. In *2016 IEEE international conference on Big data (big data)* (pp. 1412–1421).
- Maćešić, S., Črnjarić-Žic, N., & Mezić, I. (2017). Koopman operator family spectrum for nonautonomous systems – part 1. arXiv preprint arXiv:1703.07324.
- Mezić, I. (2005). Spectral properties of dynamical systems, model reduction and decompositions. *Nonlinear Dynamics*, 41(1–3), 309–325. <https://doi.org/10.1007/s11071-005-2824-x>
- Mezic, I. (2017). *Dynamics of system of systems and applications to net zero energy facilities* (Tech. Rep.). University of California-Santa Barbara Santa Barbara United States.
- Mezić, I., & Arbabi, H. (2017, December). On the computation of isostables, isochrons and other spectral objects of the koopman operator using the dynamic mode decomposition. In *International symposium on nonlinear theory and its applications*.
- Mezić, I., & Banaszuk, A. (2004). Comparison of systems with complex behavior. *Physica D: Nonlinear Phenomena*, 197(1–2), 101–133. <https://doi.org/10.1016/j.physd.2004.06.015>
- Rowley, C. W., Mezić, I., Bagheri, S., Schlatter, P., & Henningson, D. S. (2009). Spectral analysis of nonlinear flows. *Journal of Fluid Mechanics*, 641, 115–127. <https://doi.org/10.1017/S0022112009992059>
- Schmid, P. J. (2010). Dynamic mode decomposition of numerical and experimental data. *Journal of Fluid Mechanics*, 656, 5–28. <https://doi.org/10.1017/S0022112010001217>
- Williams, M. O., Kevrekidis, I. G., & Rowley, C. W. (2015, December 01). A data-driven approximation of the Koopman operator: Extending dynamic mode decomposition. *Journal of Nonlinear Science*, 25(6), 1307–1346. <https://doi.org/10.1007/s00332-015-9258-5>